Physics of Fluids

# A phase-space study of jet formation in planetary-scale fluids

Cite as: Phys. Fluids **21**, 056602 (2009); https://doi.org/10.1063/1.3140002
Submitted: 04 October 2008 . Accepted: 02 April 2009 . Published Online: 21 May 2009

R. D. Wordsworth

# A phase-space study of jet formation in planetary-scale fluids

R. D. Wordsworth[a)]
*Laboratoire de Métérologie Dynamique, Institut Pierre Simon Laplace, Paris 75252, France*

(Received 4 October 2008; accepted 2 April 2009; published online 21 May 2009)

The interaction between planetary waves and an arbitrary zonal flow is studied from a phase-space viewpoint. Using the Wigner distribution, a planetary wave Vlasov equation is derived that includes the contribution of the mean flow to the zonal potential vorticity gradient. This equation is applied to the problem of planetary wave modulational instability, where it is used to predict a fastest growing mode of finite wavenumber. A wave-mean flow numerical model is used to test the analytical predictions, and an intuitive explanation of modulational instability and jet asymmetry is given via the motion of planetary wavepackets in phase space. © *2009 American Institute of Physics*. [DOI: 10.1063/1.3140002]

## I. INTRODUCTION

The formation and maintenance of large-scale jets by the collective nonlinear interaction of eddies is a fundamental problem in planetary fluid dynamics. Perhaps the most famous example of the effect can be seen in the atmospheres of the planets Jupiter and Saturn; it has long been believed that the stable, coherent jets observed there owe their existence to continual forcing by smaller-scale eddies. Other geophysical examples of interest include Earth's atmospheric jet stream and, quite possibly, the alternating zonal jets recently observed in Earth's Pacific Ocean.[1] Further afield, an analogous effect involving plasma drift waves, is also known to be of great importance in fusion tokamaks.[2]

In all the geophysical cases, the change in planetary vorticity with latitude or $\beta$-effect is believed to be a vital part of the problem, as it allows for the presence of planetary waves in the system. In a seminal paper, Rhines[3] studied the interaction between planetary waves and turbulence, and came to the conclusion that the inverse energy cascade of idealized two-dimensional (2D) turbulence would be halted by planetary wave motion at large scales, leading to the transfer of energy into the zonal modes and hence to jet formation. Although extremely insightful, Rhines' work was partly heuristic, and could not provide a detailed dynamical explanation of the process.

As a result, the theoretical investigation of reduced problems involving the interaction of zonal jets and planetary waves is still of great importance to our overall understanding of atmospheric and oceanic fluid dynamics. Much interesting work has previously been done on the subject; for example, a number of authors have studied the interactions of planetary waves with *critical layers* in various idealized scenarios.[4–6] The foundation for many of these studies was the earlier development of various real-space conservation theorems (see, e.g., Refs. 7 and 8), most of which are now regarded as an essential part of wave-mean flow theory.

Other studies have made use of phase-space transport (Vlasov or Boltzmann) equations to describe the wave-mean flow interaction. Among the first researchers to take this approach were Dyachenko *et al.*,[9] who derived an equation for the interaction between waves and large-scale vortices. Later, Manin and Nazarenko[10] used a Vlasov equation to study the interaction between scale-separated zonal flows and planetary waves in the limit of small $\beta$-effect. They found that planetary waves in the presence of a zonal flow could become modulationally unstable, which led to singularity formation and soliton propagation in the model they used.

Recently, there have also been some attempts to utilize phase-space techniques in wave—mean flow numerical simulations. In Ref. 11, scale-separated 2D turbulence was simulated using a particle-in-cell approach. They treated the small-scale field as an ensemble of "quasiparticles" with a simple dispersion relation $\omega=\bar{\mathbf{u}}\cdot\mathbf{k}$ determined solely by the large-scale velocity field $\bar{\mathbf{u}}$. They compared their method with a direct numerical simulation, and found that it was significantly more computationally efficient.

In comparison to other approaches, however, phase-space techniques have not so far been widely used to study $\beta$-plane jet formation. One reason for this may be that often, the derived transport equations are not compatible with existing real-space results. In addition, the intuitive aspects of the phase-space view have not always been clearly emphasized, and no previous studies appear to have tested the predictions of planetary Vlasov equations against more general numerical simulations. In spite of this, the Vlasov formulation offers distinct advantages, as it allows one to build a more complete picture of interactions between arbitrary distributions of planetary waves and the mean flow than is possible with other methods. It is particularly suited to problems involving collective wave-mean flow instability, such as that considered in Sec. V of this paper.

Here, a new Vlasov equation is derived that describes the interaction of an arbitrary mean flow with a broadband distribution of scale-separated planetary waves. An operator-based derivation is used that allows all effects of the mean flow on the planetary waves to be included for the first time. It is shown that previous real-space results in wave-mean flow theory can be generalized by integrating over the Vlasov equation in spectral space. A numerical simulation is

[a)]Electronic mail: rwlmd@lmd.jussieu.fr.

 

then introduced and used to study some simple but insightful test cases involving the quasilinear motion of a planetary wavepacket. The Wigner distribution of the planetary wavefield is calculated, compared to scale-separated predictions, and used to interpret the simulation results.

Next, the modulational instability analysis of Manin and Nazarenko is generalized to include the additional potential vorticity effects of the mean flow on the waves. It is found that this generalization qualitatively changes the dispersion relation for the unstable modes. The numerical simulation is used to test the modified dispersion relation, and the development of the system beyond the initial linear growth phase is also briefly considered. In addition, it is shown that the instability process can be interpreted as a direct result of the motion of wavepackets in phase space.

In Sec. II, important results in (real-space) wave-mean flow theory for quasigeostrophic flows are reviewed. In Sec. III, the Wigner distribution is defined and used to derive a Vlasov equation for the waves. In Sec. IV, the numerical simulation is introduced. Finally, in Sec. V, the modulational instability of a planetary wave is studied using both the numerical model and the theoretical methods developed earlier.

## II. FUNDAMENTALS OF WAVE-MEAN FLOW THEORY

The key features of many large-scale geophysical flows can be captured by the quasigeostrophic potential vorticity (QGPV) equation

$$\frac{Dq}{Dt} = \frac{\partial q}{\partial t} + J[\psi, q] = -\kappa q, \tag{1}$$

where $\psi$ is the velocity stream function, $q=\{\partial_{xx}+\partial_{yy}+\partial_z[(f_0^2/N^2)\partial_z]\}\psi+\beta y$ is the QGPV, $\beta$ is the local gradient of planetary vorticity with latitude, $J[,]$ is the 2D Jacobian operator such that $J[f,g]=\partial_x f\partial_y g-\partial_x g\partial_y f$ in Cartesian coordinates, and $\kappa$ is the Ekman damping parameter. In the definition of $q$, the constant $f_0$ is the Coriolis parameter and $N$ is the buoyancy frequency, which in standard quasigeostrophic theory is a function of $z$ only.

Equation (1) is simply a statement that $q$ is conserved following fluid elements in the absence of damping and forcing. It is an approximation to the full Navier–Stokes equations that is applicable when the system under consideration is rapidly rotating and strongly stratified, and is derived in detail in many fluid dynamics textbooks (see, e.g., Ref. 12). For convenience, in this paper we work with Eq. (1) in Cartesian coordinates according to the standard $\beta$-plane model (see Fig. 1). We also mostly focus on the situation where the system is unbounded in the $y$ (north-south) direction, although in Sec. V, the north-south boundary conditions are set to be periodic for simplicity. The theoretical setup is summarized in Fig. 1.

As a result of the background vorticity gradient $\beta$, the linearized form of Eq. (1) has planetary wave solutions, with dispersion relation

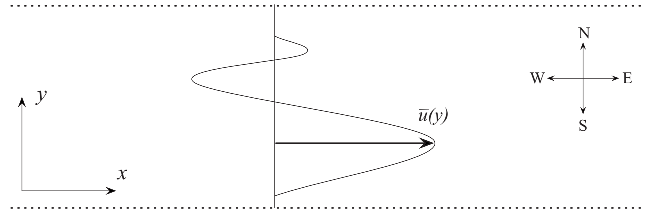


FIG. 1. Schematic of the theoretical setup: a $\beta$-plane model periodic in the $x$-direction and open in the $y$-direction. The $\beta$-plane approximates fluid motion on the midlatitudes of a planet, with $x$ and $y$ equivalent to east-west and north-south directions, respectively.

$$\sigma = \frac{-\beta k_x}{k_x^2 + k_y^2 + k_z^2} \tag{2}$$

when no zonal flow or damping is present. In Eq. (2), $k_z$ is understood to be an eigenvalue of the usual vertical structure equation such that $\partial_z[(f_0^2/N^2)\partial_z\Psi]=-k_z^2\Psi$, subject to suitable boundary conditions.

To investigate the interaction between planetary waves and zonal flow, it is standard to define an average in the $x$-direction such that any quantity decomposes into a mean flow and a disturbance field: $f(x,y,t)=\overline{f(y,t)}+f'(x,y,t)$. Then, Eq. (1) becomes

$$\frac{\partial \bar{q}}{\partial t} = -\frac{\partial}{\partial y}\overline{v'q'} - \kappa \bar{q} \tag{3}$$

for the mean flow and

$$\frac{\partial q'}{\partial t} + \bar{u}\frac{\partial q'}{\partial x} + \gamma v' = \overline{J[\psi',q']} - J[\psi',q'] - \kappa q' \tag{4}$$

for the disturbances, with $\gamma=\partial_y\bar{q}$ the total gradient of zonal potential vorticity. The left hand side of Eq. (4) describes the evolution of planetary waves in the presence of a zonal flow, while the right describes nonconservative effects and wave-wave interactions.

As this work is primarily concerned with wave-mean flow interaction, we will assume the wave-wave terms in Eq. (4) to be small from here onward. In Sec. IV, where we discuss the numerical simulation of a generic jet-wave interaction problem, the situations where this assumption begins to fail will be made clear.

For moderate disturbance amplitudes, it can be shown that the *wave action*, defined as $n\equiv\frac{1}{2}\overline{q'^2}/\gamma$, is a conserved quantity. This can be seen through multiplication of Eq. (4) by $q'/\gamma$ and zonal averaging, which results in

$$\frac{\partial n}{\partial t} + \overline{v'q'} = -2\kappa n \tag{5}$$

if terms of order $q'^3$ and greater are neglected. If spatial scale separation between zonal flow and waves is then assumed and the waves are taken to be monochromatic, a real-space transport equation for wave action can be written,

$$\frac{\partial n}{\partial t} + \nabla_m \cdot (\mathbf{v}_m n) = -2\kappa n, \tag{6}$$

where $\nabla_m = (\partial_y, \partial_z)$ and $\mathbf{v}_m$ is the meridional $(y,z)$ group velocity of the waves. For further details of the derivation of Eq. (5), see Ref. 13.

Note that the definition of $n$ given here depends on the potential vorticity gradient, $\gamma$, remaining nonzero. If $\gamma$ changes sign somewhere in the domain, then the zonal flow may be unstable. The problems associated with defining $n$ in these cases are discussed in more detail in Ref. 14.

The final established result of importance to the rest of this paper is the powerful *nonacceleration theorem*, which states that in the absence of forcing or damping, the rate of change in zonal potential vorticity and wave action are directly tied to each other,

$$\frac{\partial}{\partial t}\left(\bar{q} - \frac{\partial n}{\partial y}\right) = 0. \tag{7}$$

Equation (7) can be proved by use of the Taylor identity,[13] or by combining Eqs. (3) and (5) and setting $\kappa = 0$.

## III. DERIVATION OF THE PLANETARY WAVE VLASOV EQUATION

In this section, we generalize the results reviewed in Sec. II to arbitrary broadband distributions of planetary waves. As was mentioned in Sec. I, equations for broadband wave-mean flow interaction have been used in several previous studies. The aim here is to derive a Vlasov equation that is directly compatible with the real-space wave-mean results reviewed in Sec. II. As will be shown, this requires the inclusion of additional mean flow effects that qualitatively change the predictions, particularly in the modulational instability analysis of Sec. V.

We begin the derivation by writing the disturbance equation (4) in terms of a new variable $\phi \equiv q'/\sqrt{2\gamma}$. If we neglect terms of order $\phi^2$ and higher, Eq. (4) then takes the form

$$i\frac{\partial \phi}{\partial t} = \hat{G}\phi, \tag{8}$$

where the wave operator $\hat{G}$ is defined as

$$\hat{G}[\hat{\mathbf{x}}, \hat{\mathbf{k}}, t] \equiv \sqrt{\gamma}\frac{-\hat{k}_x}{\hat{k}_x^2 + \hat{k}_y^2 + \hat{k}_z^2}\sqrt{\gamma} + \bar{u}\hat{k}_x - i\kappa. \tag{9}$$

Note that $\hat{G}$ is a self-adjoint operator when the damping term $\kappa = 0$. This is part of the motivation for introducing the "square root of wave action" variable $\phi$. As will be seen later, our choice of $\phi$ is also very important in ensuring that the new results correctly generalize the real-space wave action equation (6).

The position and wavevector operators are

$$\hat{\mathbf{x}} = \mathbf{x} \quad \text{and} \quad \hat{\mathbf{k}} = \{-i\partial_x, -i\partial_y, -i\sqrt{\partial_z[(f_0^2/N^2)\partial_z]}\}, \tag{10}$$

respectively, as we are working in a position space representation. The denominator in Eq. (9) is simply the potential vorticity inversion operator, such that

$$\psi = -(\hat{k}_x^2 + \hat{k}_y^2 + \hat{k}_z^2)^{-1} q = [\partial_{xx} + \partial_{yy} + \partial_z(f_0^2/N^2)\partial_z]^{-1} q. \tag{11}$$

When scale separation *is* assumed, operators become real numbers, and the large-scale zonal flow "sees" wavepackets as phase-space points with exact values of $\mathbf{x}$ and $\mathbf{k}$. Then, Eq. (9) simply becomes the generalized dispersion relation for small-scale planetary waves in the presence of a zonal flow and damping

$$\hat{G}[\hat{\mathbf{x}}, \hat{\mathbf{k}}, t] \to \omega(y,z,\mathbf{k},t) = \frac{-\gamma k_x}{k_x^2 + k_y^2 + k_z^2} + \bar{u}k_x - i\kappa. \tag{12}$$

At this point, we need to utilize a tool from quantum mechanics: the Wigner distribution. It is defined in three dimensions as

$$\mathcal{N}_{\phi,\phi}(\mathbf{x},\mathbf{k},t) = \frac{1}{(2\pi)^3}\int_{-\infty}^{+\infty} \phi^*_{\mathbf{x}-(1/2)\mathbf{x}_1} e^{-i\mathbf{k}\cdot\mathbf{x}_1} \phi_{\mathbf{x}+(1/2)\mathbf{x}_1} d^3\mathbf{x}_1, \tag{13}$$

or alternatively in spectral space as

$$\mathcal{N}_{\phi,\phi}(\mathbf{x},\mathbf{k},t) = \frac{1}{(2\pi)^3}\int_{-\infty}^{+\infty} \Phi^*_{\mathbf{k}-(1/2)\mathbf{k}_1} e^{i\mathbf{x}\cdot\mathbf{k}_1} \Phi_{\mathbf{k}+(1/2)\mathbf{k}_1} d^3\mathbf{k}_1, \tag{14}$$

where $\Phi(\mathbf{k},t) = (2\pi)^{-3/2}\int_{-\infty}^{+\infty}\exp[-i\mathbf{k}\cdot\mathbf{x}]\phi(\mathbf{x},t)d^3\mathbf{x}$ is the Fourier transform of $\phi$. $\mathcal{N}_{\phi,\phi}$ can broadly be thought of as a phase-space distribution for the function $\phi$, but it has some fairly weird properties—not least of which being that it can take *negative* values. However, its projections onto real and spectral space are always positive valued.

By taking a time derivative of Eq. (13) and using Eq. (8), we may write

$$i\frac{\partial \mathcal{N}_{\phi,\phi}}{\partial t} = \mathcal{N}_{-\hat{G}\phi,\phi} + \mathcal{N}_{\phi,\hat{G}\phi}. \tag{15}$$

Then, by defining the *phase-space* operators $\hat{\mathbf{X}} = \mathbf{x} + i/2\nabla_{\mathbf{k}}$ and $\hat{\mathbf{K}} = \mathbf{k} - i/2\nabla_{\mathbf{x}}$ (see, e.g., Ref. 15) and noting that

$$\hat{\mathbf{X}}\mathcal{N}_{\phi,\phi} = \mathcal{N}_{\phi,\hat{\mathbf{x}}\phi}, \quad \hat{\mathbf{K}}\mathcal{N}_{\phi,\phi} = \mathcal{N}_{\phi,\hat{\mathbf{k}}\phi}, \tag{16}$$

and hence clearly

$$\hat{\mathbf{X}}^n\mathcal{N}_{\phi,\phi} = \mathcal{N}_{\phi,\hat{\mathbf{x}}^n\phi}, \quad \hat{\mathbf{K}}^n\mathcal{N}_{\phi,\phi} = \mathcal{N}_{\phi,\hat{\mathbf{k}}^n\phi}, \tag{17}$$

the fairly weak assumption that $\hat{G}[\hat{\mathbf{X}}, \hat{\mathbf{K}}, t]$ can be expanded in powers of the two operators $\hat{\mathbf{X}}$ and $\hat{\mathbf{K}}$ (i.e., that it has a valid Taylor series representation) allows us to arrive at

$$i\frac{\partial \mathcal{N}_{\phi,\phi}}{\partial t} = (\hat{G}[\hat{\mathbf{X}}, \hat{\mathbf{K}}, t] - \hat{G}[\hat{\mathbf{X}}^*, \hat{\mathbf{K}}^*, t])\mathcal{N}_{\phi,\phi}. \tag{18}$$

Equation (18) is the Wigner transport equation, describing the motion of planetary wave action in phase space without an assumption of scale separation. Although it is general, its form is based on operator notation, which unfortunately makes direct analysis difficult. Therefore, we derive the Vlasov equation via a Taylor expansion of the operator $\hat{G}$ about

$\mathbf{x}$ and $\mathbf{k}$. Truncation of the expansion at first order allows us to write

$$\hat{G}[\hat{\mathbf{X}},\hat{\mathbf{K}},t] \approx \omega(\mathbf{x},\mathbf{k},t) + \frac{\partial \omega}{\partial \mathbf{x}} \cdot \frac{i}{2}\frac{\partial}{\partial \mathbf{k}} - \frac{\partial \omega}{\partial \mathbf{k}} \cdot \frac{i}{2}\frac{\partial}{\partial \mathbf{x}}. \quad (19)$$

Provided that such a representation for $\hat{G}$ is valid, a similar expansion for $\hat{G}[\hat{\mathbf{X}}^*,\hat{\mathbf{K}}^*,t]$ and substitution into Eq. (18) then leads to

$$\frac{\partial \mathcal{N}}{\partial t} + \mathbf{v} \cdot \frac{\partial \mathcal{N}}{\partial \mathbf{x}} + \mathbf{F} \cdot \frac{\partial \mathcal{N}}{\partial \mathbf{k}} = \Gamma[\mathcal{N}], \quad (20)$$

where $\mathbf{v}$ and $\mathbf{F}$, the group velocity of, and force on, a wavepacket, respectively, have their usual definitions as $\mathbf{v}=\nabla_{\mathbf{k}}\omega$ and $\mathbf{F}=-\nabla_{\mathbf{x}}\omega$. For brevity, we write $\mathcal{N}_{\phi,\phi}=\mathcal{N}$ from here.

Equation (20) is equivalent to Eq. (18) in the geometrical optics limit of small-scale disturbances. It describes the collective motion of an ensemble of pointlike wavepackets through phase space. The right hand side of Eq. (20) contains all nonconservative terms: According to our derivation, $\Gamma[\mathcal{N}]=-2\kappa\mathcal{N}$. However, if the effects of wave-wave interactions were to be included, $\Gamma$ would also contain more complicated terms describing collisions between wavepackets. For the general case of planetary waves on an arbitrary zonal flow, these terms are not known. They were derived for small-scale planetary wave interaction in the *absence* of zonal flow by several authors, beginning with Longuet-Higgins and Gill.[16] As the interaction of planetary waves is well known to be incapable of giving energy to the zonal flow at lowest order, and our main interest is the interaction between waves and zonal flow, we will not make use of these results here.

Differentiation of Eq. (12) in phase space yields the group velocities and rates of change of wavenumber or "forces" on planetary wavepackets,

$$\mathbf{v} = \left( -\frac{\gamma}{|\mathbf{k}|^2} + \bar{u} + \frac{2\gamma k_x^2}{|\mathbf{k}|^4}, \frac{2\gamma k_x k_y}{|\mathbf{k}|^4}, \frac{2\gamma k_x k_z}{|\mathbf{k}|^4} \right)$$
$$\mathbf{F} = \left( 0, \frac{k_x}{|\mathbf{k}|^2}\frac{\partial \gamma}{\partial y} - k_x \frac{\partial \bar{u}}{\partial y}, \frac{k_x}{|\mathbf{k}|^2}\frac{\partial \gamma}{\partial z} - k_x \frac{\partial \bar{u}}{\partial z} \right), \quad (21)$$

with $|\mathbf{k}|^2=k_x^2+k_y^2+k_z^2$ and $\mathbf{v}=d\mathbf{x}/dt$, $\mathbf{F}=d\mathbf{k}/dt$.

Finally, if we *define* the wave action $n$ [see Eq. (5)] to be the projection of $\mathcal{N}$ onto $(y,z)$ real space

$$n(y,z,t) \equiv \overline{\int_{-\infty}^{+\infty} \mathcal{N}(\mathbf{x},\mathbf{k},t) d^3\mathbf{k}}, \quad (22)$$

where the overline denotes the zonal average defined earlier, we can extend the results of standard wave-mean flow theory outlined in Sec. II. By integrating Eq. (20) over $\mathbf{k}$, making use of the fact that $\nabla_{\mathbf{x}}\cdot\mathbf{v}+\nabla_{\mathbf{k}}\cdot\mathbf{F}=0$ and assuming that $\mathcal{N}\to 0$ as $|\mathbf{k}|\to\infty$, we arrive at

$$\frac{\partial n}{\partial t} + \nabla_{2D}\cdot(\langle \mathbf{v}_{2D}\rangle n) = -2\kappa n, \quad (23)$$

where

$$\langle \mathbf{v}_{2D}\rangle \equiv \overline{\frac{1}{n}\int_{-\infty}^{+\infty} \mathbf{v}\mathcal{N} d^3\mathbf{k}} \quad (24)$$

is the spectrally averaged $(y,z)$ group velocity for the planetary waves. Equation (23) is a generalization of Eq. (6) to a broadband distribution of small-scale waves, which is made possible by the initial definition of $\phi$, not $q'$, as the quantity in the wave equation (8). Interestingly, its derivation from Eq. (20) is closely analogous to the derivation of the continuity equation from the Boltzmann equation in fundamental fluid dynamics.

## IV. NUMERICAL SIMULATION I: MOTION OF A SINGLE WAVEPACKET

We now wish to develop a more intuitive understanding of the ideas of the previous section, by considering a wave-mean flow numerical simulation. The simple test cases studied here are interesting in their own right, but they are also important for the phase-space interpretation of planetary wave modulational instability, which is discussed in Sec. V.

The essential features of the wave-mean flow problem are captured by restricting the planetary wavefield to a single east-west wavenumber, $k_x=k_0$, but allowing it to be broadband in $k_y$. This is justified by noting that according to Eq. (21), the zonal flow cannot move the planetary wavepackets to different $k_x$ and also that in a wave-mean flow context, their $x$-position is clearly irrelevant. For simplicity we also ignore damping ($\kappa=0$), and restrict the problem to the single layer *barotropic* case. However, it should be noted that all of the theory presented in the previous section is also applicable to mixed barotropic/baroclinic flows, which in general will vary with height as well as latitude and longitude.

For barotropic planetary waves, only the $y$ and $k_y$ dimensions of phase space are of relevance. In particular, the equation for phase-space velocity vectors (21) simplifies to the two components,

$$v_y = \frac{2\gamma k_x k_y}{|\mathbf{k}|^4}, \quad F_y = \frac{k_x}{|\mathbf{k}|^2}\frac{\partial \gamma}{\partial y} - k_x\frac{\partial \bar{u}}{\partial y}. \quad (25)$$

To investigate Eqs. (3) and (4) numerically, we write the disturbance vorticity as $q'=\mathrm{Re}[Qe^{ik_0x}]$, allowing the derivation of the simplified equations,

$$i\frac{\partial Q}{\partial t} = k_0(\bar{u}Q + \gamma\Psi) - i\kappa Q, \quad \hat{\Psi} \equiv -(\hat{k}_y^2 + k_0^2)^{-1}Q \quad (26)$$

and

$$\frac{\partial \bar{u}}{\partial t} = \overline{v'q'} - \kappa\bar{u} = -\frac{k_0}{2}(\mathrm{Im}[\Psi]\mathrm{Re}[Q] - \mathrm{Im}[Q]\mathrm{Re}[\Psi]) - \kappa\bar{u} \quad (27)$$

for waves and mean flow, respectively. It should be emphasized at this point that $\hat{k}_y=-i\partial_y$ is an operator, as defined in Eq. (10), and hence Eqs. (26) and (27) make no assumption of scale separation.

For all the numerical results presented here, Eqs. (26) and (27) were solved using an explicit fourth order Runge–Kutta method. The program was designed to halt whenever

(a) the Rayleigh–Kuo criterion $\beta-\bar{u}''<0$ for barotropic instability or (b) the heuristic wave-breaking criterion $|u'|_{max}>\omega/k_x$ were satisfied. This ensured that the original physical assumptions behind the model were not broken during the simulation.

As this simulation is highly idealized and not intended to directly model real planetary flows, dimensionless units are used throughout this section. For comparison, however, we note that for a midlatitude slice of Jupiter's atmosphere, when scaled into units of planetary rotation period $T_J$ and radius $r_J$, the mean zonal wind speed is approximately $\bar{u}=0.01r_JT_J^{-1}$ and the $\beta$ parameter is $\beta=5-10r_J^{-1}T_J^{-1}$, depending on latitude. For all simulations in this section we used $\beta=10$, and maximum zonal wind speeds of barotropically stable jets were of order $\max[\bar{u}]=0.001$. Thus we are investigating a fluid dynamical regime with slightly weaker zonation, generally, than that observed on the gas giant planets.

First, we study an extremely simple test case: a near-infinitesimal wavepacket with no initial zonal flow and no Ekman damping. The initial disturbance vorticity is

$$Q=Q_0\exp[il_0y-(y-y_0)^2/(\Delta y)^2], \tag{28}$$

with $l_0=k_0=60$, $y_0=0.25$, and $\Delta y=0.1$. In Fig. 2, the magnitude of the Wigner distribution $|\mathcal{N}_{\phi,\phi}|$ is plotted above zonal velocity $\bar{u}$ for a series of time steps. For all the plots in this section, $\mathcal{N}_{\phi,\phi}$ was calculated directly from the numerical eddy vorticity, without any scale separation assumption.

As can be seen, when the wavepacket has wavevector such that $k_xk_y>0$, it drifts northward due to the $\beta$-effect. Weak zonal jets form as a result of this motion. By the barotropic version of the nonacceleration theorem (7),

$$\frac{\partial\bar{u}}{\partial t}=-\frac{\partial n}{\partial t}, \tag{29}$$

we see that latitudinal planetary wavepacket motion must always cause jets to form in this way. This process is summarized in Fig. 3.

The group velocity calculated from Eq. (25) agrees closely with the observed velocity of the wavepacket peak (the difference is less than 3% in the example shown). However, note the stretching of the wavepacket in phase space due to the dispersive nature of the planetary waves, as determined by Eq. (2). Essentially, the local group velocity $v_y$ on the left hand side (in phase space) of the wavepacket is greater than that on the right—this is shown by the arrows on the first plot in Fig. 2.

The second basic case of interest involves an infinitesimal wavepacket on a linearly sheared zonal flow of the form $\bar{u}=-\Lambda(y-y_0)$. Here, $\Lambda=0.01$, $y_0=0.5$, and all other parameters are as in the previous example. As shown in Fig. 4, in this situation a wavepacket with $k_x>0$ is forced towards higher $k_y$ wavenumbers, losing energy to the zonal flow in the process. As $\beta=\gamma$ in this example, the enstrophy of the wavepacket remains constant and hence energy is transferred upscale, while enstrophy moves downscale. Again, scale-separated predictions match the observed value closely for this case.

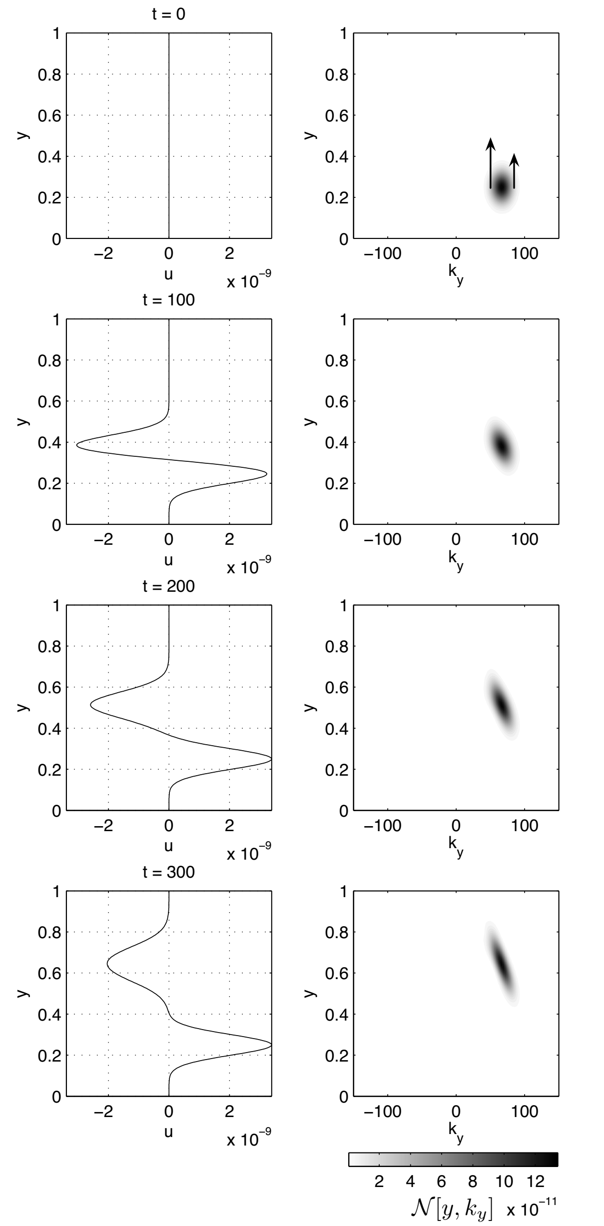


FIG. 2. A planetary wavepacket on a $\beta$-plane with positive $k_y$ and $k_y$ will move northward. As group velocity depends on $k_y$, the wavepacket becomes tilted in phase space (second column), although its volume remains approximately the same. Note the small-amplitude zonal flow (first column) induced by the wavepacket motion.

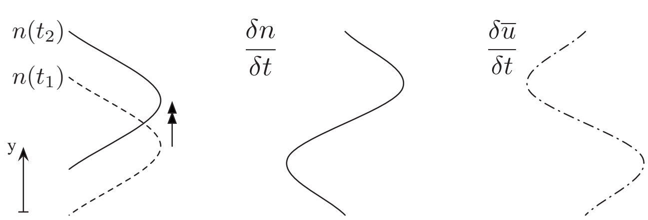


FIG. 3. Schematic explanation of the jet formation seen in Fig. 2. If a planetary wavepacket is moving northwards such that in time $\delta t=t_2-t_1$, $\delta n=n(t_2)-n(t_1)$, then the nonacceleration theorem (29) ensures the zonal flow produced $\delta\bar{u}$ will be of the form shown.

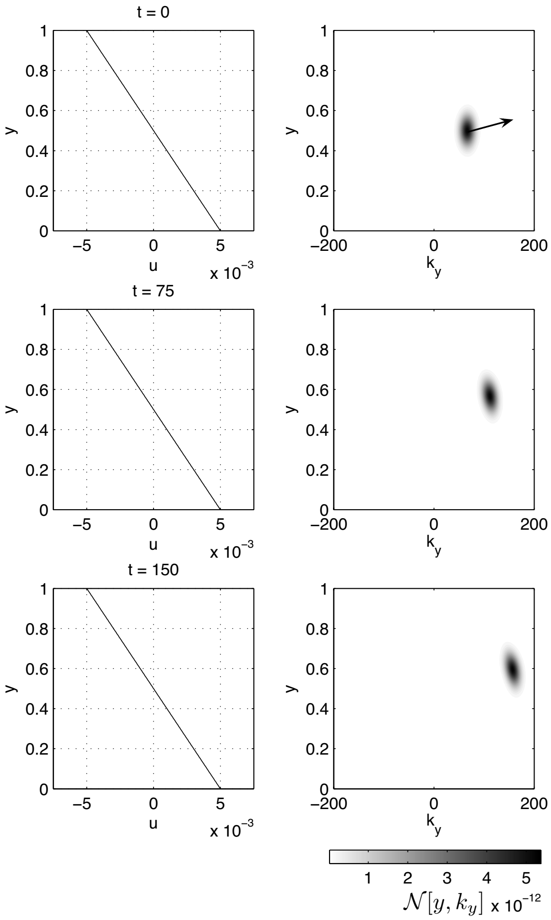


FIG. 4. In the presence of a shear flow that decreases linearly with latitude (far left), a planetary wavepacket with positive $k_x$ will move toward higher wavenumbers, losing energy to the zonal flow in the process. Note the slight northward drift of the wavepacket; this is due to the $\beta$-effect shown in Fig. 2.

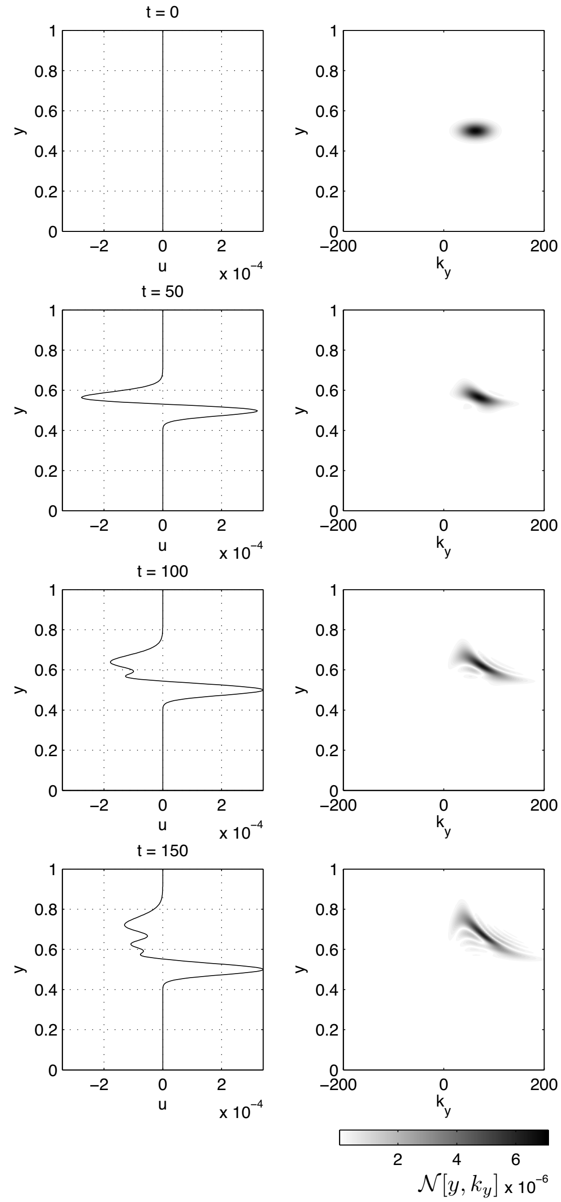


FIG. 5. Quasilinear evolution of a wavepacket ($Q_0$=0.12, $y_0$=0.5, $\Delta y$=0.05, all other parameters as in first example). Initially, the wavepacket moves as in Fig. 2, but the zonal shear it produces modifies its motion as time progresses. Note that by $t$=100, the Wigner distribution has become negative valued in places.

More interesting and subtle phenomena occur when we allow the wavepacket to be of large enough amplitude for coupling with the zonal flow, but not wave breaking, to occur (see Fig. 5). Then, we expect it to initially move northward, with two zonal jets forming due to the nonacceleration theorem, as in the first example. However, as the zonal flow becomes stronger, it begins to influence wavepacket propagation through (a) the shear effect described in the second example and (b) alteration of the basic potential vorticity gradient $\gamma=\beta-\partial_{yy}\bar{u}$ [see Eq. (25)]. As the initial zonal flow gradient in the center of the channel is negative, the wavepacket is forced to higher $k_y$ wavenumbers, reducing its group velocity and hence the growth rate of the zonal flow. This process continues until the zonal flow either removes most of the wavepacket energy and reaches a quasisteady state, or sharpens to the extent that it becomes barotropically unstable.

Interestingly, the same east-west jet asymmetry occurs regardless of the wavevector **k** sign of the initial wavepacket. As expected from Eq. (25) and shown in Fig. 6, if the product $k_xk_y$ is negative, the wavepacket initially moves south, and the initial induced jets are of opposite sign. However, whatever the sign of $k_x$ and $k_y$, jet formation always pushes some wave action to higher *absolute* wavenumber values $|k_y|$. Combined with the fact that the wavepacket propagates away from the jet in a direction dependent on $k_xk_y$, the result is that in each case, the eastward jet becomes sharper than the westward one.

Evidence of quasigeostrophic jet asymmetry has been found in several previous numerical studies (e.g., Refs. 17–19). Indeed, east-west asymmetry appears to be a quite generic feature of wave-forced jets on the $\beta$-plane. The examples given here simply demonstrate the intuitive explanation of the phenomenon that is possible from a phase-space viewpoint.

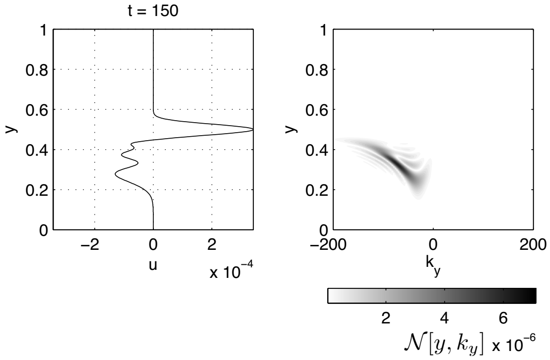


FIG. 6. State at $t=150$ of the same simulation as Fig. 5, but with the initial $k_y$ value of the wavepacket reversed.

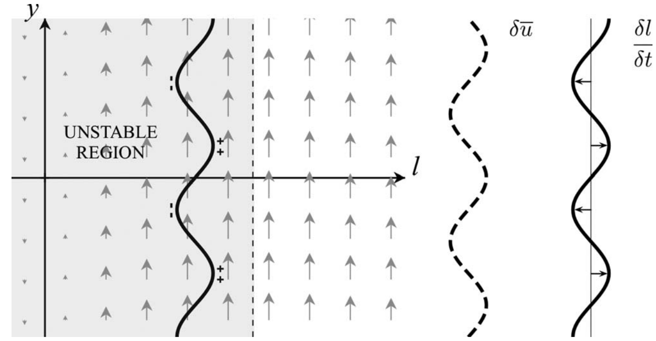


FIG. 7. Phase-space interpretation of the instability criterion (35). Gray arrows show local wavepacket velocity when no mean flow is present. The plus (minus) signs denote regions where wavepackets accelerate (decelerate) relative to the base group velocity $v_{0y}$. The mean flow response $\delta\bar{u}$ and resulting motion of wavepackets in the $l$-direction $\delta l/\delta t$ are also shown.

## V. NUMERICAL SIMULATION II: MODULATIONAL INSTABILITY

In this section, we use Eq. (20) and the numerical model just described to study the important problem of planetary wave modulational instability. While it has been known in principle that systems of planetary waves are unstable to modulations since at least the study of Newell[20] (see also the related reference[21]), the phenomenon has received less attention to date in planetary fluid dynamics than it perhaps deserves. In Ref. 22 the *longitudinal* instability of planetary waves was studied as a means to explain extratropical wavepacket formation. However, the geometry of the problem meant that zonal jet formation did not occur as a result. Manfroi and Young[23] used the weakly nonlinear formulation of Sivashinsky[24] to study a more related problem involving the instability of a stationary planetary mode in the presence of bottom drag and viscosity. They found that asymmetric jets formed in their model, with an average separation that was dependent on the bottom drag.

The most relevant work to this section, however, is the previously cited Manin and Nazarenko,[10] in which a Vlasov equation similar to Eq. (20) was used to study the latitudinal instability of planetary waves in the limit of small $\beta$-effect. Here, we begin by summarizing their methods and the result of their instability calculation. We then show how their calculation can be generalized using the results of Sec. III. It is found that inclusion of the mean flow correction terms results in a qualitatively different prediction for the fastest growing modes. The new instability predictions are then compared to results from the numerical model introduced in Sec. IV. As in Sec. IV, the vertical variation of all quantities is neglected here.

To reduce their mean flow equation into a tractable form, Manin and Nazarenko assumed that the wavepacket density $\mathcal{N}$ could be treated as a $\delta$-function in wavenumber space dependent on a single dynamical variable $l(y,t)$

$$\mathcal{N}(\mathbf{x},\mathbf{k}',t)=\mathcal{N}_0\delta(k'-k_0)\delta[l'-l(y,t)]. \tag{30}$$

When this assumption is applied to Eqs. (23) and (29) with $\kappa=0$, the result is

$$\frac{\partial\bar{u}}{\partial t}=\mathcal{N}_0\frac{\partial v_y}{\partial y}. \tag{31}$$

Equation (31) combined with the previous definition of force on a wavepacket

$$\frac{\partial l}{\partial t}=F_y=-\frac{\partial\omega}{\partial y}, \tag{32}$$

then completely describes the evolution of the reduced system.

To find a dispersion relation for the modulational instability of a monochromatic wave, it is necessary to linearize Eqs. (31) and (32) about a single wavenumber value $l=l_0+\tilde{l}$, $\bar{u}=\tilde{u}$, with $\tilde{l},\tilde{u}\propto\exp(-iK+i\Omega)$. In the work of Manin and Nazarenko, the analysis was further simplified by earlier assumptions that (a) the local planetary wave group velocity is only a function of $\beta$, not $\gamma$ and (b) the Doppler term $k_0\bar{u}$ [see Eq. (12)] dominates all others in $\omega$.

In these circumstances, $v_y$ can be expanded in terms of $\tilde{l}$ only, and the dispersion relation for the modulational instability can be written as

$$\Omega=\pm iK\sqrt{\mathcal{N}_0k_0\left.\frac{\delta v_y}{\delta l}\right|_{l=l_0}}, \tag{33}$$

where

$$\left.\frac{\delta v_y}{\delta l}\right|_{l=l_0}=\frac{2k_0\beta(k_0^2-3l_0^2)}{(k_0^2+l_0^2)^3}. \tag{34}$$

Clearly, Eq. (33) predicts the most unstable wave will always be the one of highest wavenumber $K$. It also predicts that a wave will only become unstable if

$$k_0^2/l_0^2>3. \tag{35}$$

The instability criterion (35) has an intuitive phase-space interpretation, which is visualized in Fig. 7. When a monochromatic planetary wave (equivalently, a thin phase-space strip of wave action) is perturbed in the $l$-direction, the gradient of base group velocity $v_{0y}$ (see Fig. 2) causes a convergence of wave action into certain regions and a divergence out of others. By the nonacceleration theorem, local wave action

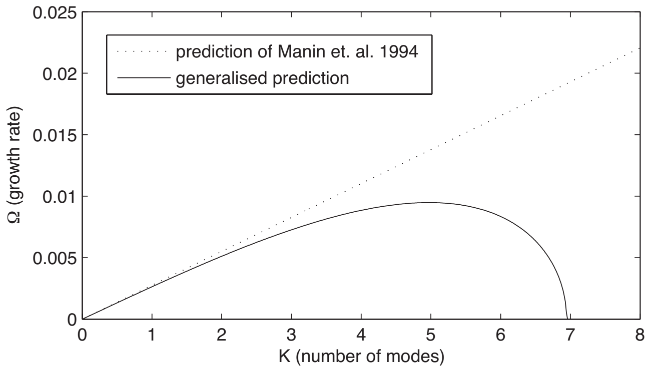


FIG. 8. Growth rate as a function of mode number for the prediction of Manin and Nazarenko [Eq. (33)] and the generalized instability criterion (37).

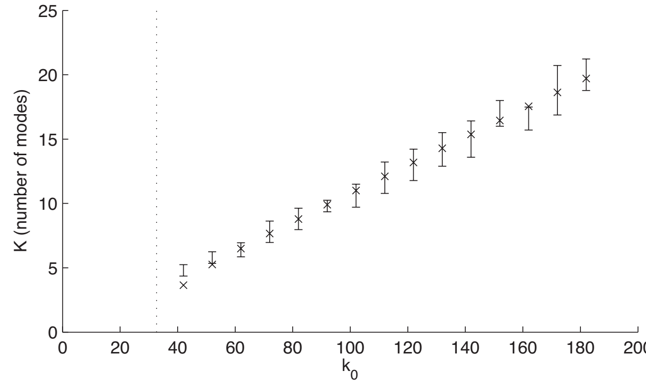


FIG. 9. Theoretically predicted fastest growing mode (crosses) and most energetic zonal modes at onset of barotropic instability in simulation (error bars). Dotted line shows critical $k_0$ value as given by Eq. (35).

changes must cause an equal and opposite change in the local zonal velocity $\bar{u}$. In the unstable region of phase space (shaded gray in Fig. 7), the gradient of group velocity is such that this zonal velocity then causes the initial perturbation to grow via the shear effect discussed in Sec. IV (see Fig. 4). After the linear growth phase, the convergence of positive wave action into certain regions must cause the associated negative zonal jets to intensify. Thus jet asymmetry in the *opposite sense* to that seen in Sec. IV is expected to develop in this example.

If the two assumptions of Manin and Nazarenko are not used, the instability analysis becomes more complicated. Multiple variable Taylor expansions of $\omega$ and $v_y$ yield

$$i\Omega\tilde{u} = -iK\mathcal{N}_0\left(\left.\frac{\delta v_y}{\delta l}\right|_0 \tilde{l} + \left.\frac{\delta v_y}{\delta \bar{u}}\right|_0 \tilde{u}\right),$$

$$i\Omega\tilde{l} = +iK\left(\left.\frac{\delta\omega}{\delta\bar{u}}\right|_0 \tilde{u} + \left.\frac{\delta\omega}{\delta l}\right|_0 \tilde{l}\right), \tag{36}$$

and hence

$$\Omega = \frac{1}{2}K\left[V \pm \sqrt{V^2 - 4\mathcal{N}_0\left(\left.\frac{\delta v_y}{\delta l}\right|_0 \left.\frac{\delta\omega}{\delta\bar{u}}\right|_0 - v_{0y}\left.\frac{\delta v_y}{\delta\bar{u}}\right|_0\right)}\right]. \tag{37}$$

Here $V = v_{0y} - \mathcal{N}_0(\delta v_y/\delta\bar{u})|_0$ is the wavepacket velocity at $l = l_0$ with a correction due to mean flow effects. The explicit forms of the partial derivatives are

$$\left.\frac{\delta\omega}{\delta\bar{u}}\right|_0 = \frac{-k_0K^2}{k_0^2+l_0^2} + k_0, \qquad \left.\frac{\delta\omega}{\delta l}\right|_0 = v_{0y} = \frac{2k_0l_0\beta}{(k_0^2+l_0^2)^2},$$

$$\left.\frac{\delta v_y}{\delta\bar{u}}\right|_0 = \frac{2k_0l_0K^2}{(k_0^2+l_0^2)^2}, \qquad \left.\frac{\delta v_y}{\delta l}\right|_0 = \frac{2k_0\beta(k_0^2-3l_0^2)}{(k_0^2+l_0^2)^3}, \tag{38}$$

where $|_0$ implies evaluation at $l = l_0$ and $\bar{u} = 0$. The mean flow corrections in Eq. (38) are negligible for small $K$. At high $K$ values, however, they become increasingly important, with the result that imaginary part of $\Omega(K)$ has a definite maximum, after which it decreases to zero. In Fig. 8, Eqs. (33) and (37) are plotted as function of $K$ for an example where $k_0 = 50$, $l_0 = 6\pi$, $\beta = 1$, and $\mathcal{N}_0 = 6\times10^{-4}$. As can be seen, their predictions diverge at high $K$ values, with the latter peaking at approximately $K = 5$ modes. Equation (37) gives a maximum $\Omega(K)$ value at finite $K$ in a similar way for all cases where criterion (35) is satisfied.

To test the validity of this scale-separated analysis, we now compare its predictions with the results of numerical simulation. The setup is very similar to that used in Sec. IV. One exception is the boundary conditions in the $y$-direction, which are now set to be periodic, for simplicity. Strictly speaking, the derivation of Sec. III is only valid for unbounded domains, but we expect that it should still work reasonably well as long as the wavelength of any energetic modes in the system are several times less than the latitudinal domain size, $\lambda_{max} < L_y$. In each simulation, the initial condition consists of a planetary wave of definite wavenumbers $k_0$ and $l_0$, plus a small amount of random noise. The system is allowed to evolve until the Rayleigh–Kuo criterion $\beta - \partial_{yy}\bar{u} > 0$ is violated, and then the wavenumber of the most energetic zonal mode is determined via a Fourier transform.

In Fig. 9, the results of many such simulations, performed for varying values of $k_0$, are plotted alongside theoretical predictions. All other quantities were fixed at the same values as those for Fig. 8. As the largest mode in the simulation was found to vary unpredictably over a given range for each $k_0$ value, it was decided to perform five simulations at each point. It is the standard deviation about the average mode number that is plotted in Fig. 9. Resolution in the $y$-direction was set at $ny = 128$; increasing this value did not significantly affect the results.

As can be seen, Eq. (37) accurately predicts the fastest growing mode at most values of $k_0$, with the variation nearly linear above the critical $k_0$ value. The reason for the slight divergence at low $k_0$ is not known; it is possible that the periodic boundary conditions or other nonlocal effects played a role in these cases. The dependence of the prediction on $l_0$ was also tested; it was found that even for the extreme case $l_0 = 0$, the agreement between theory and simulation was fairly close. Finally, the variation with $\mathcal{N}_0$ was tested, and it was found that both the predicted and simulated fastest growing modes remained almost constant with $\mathcal{N}_0$ over fairly large ranges.

In general, this analysis predicts a fastest growing zonal

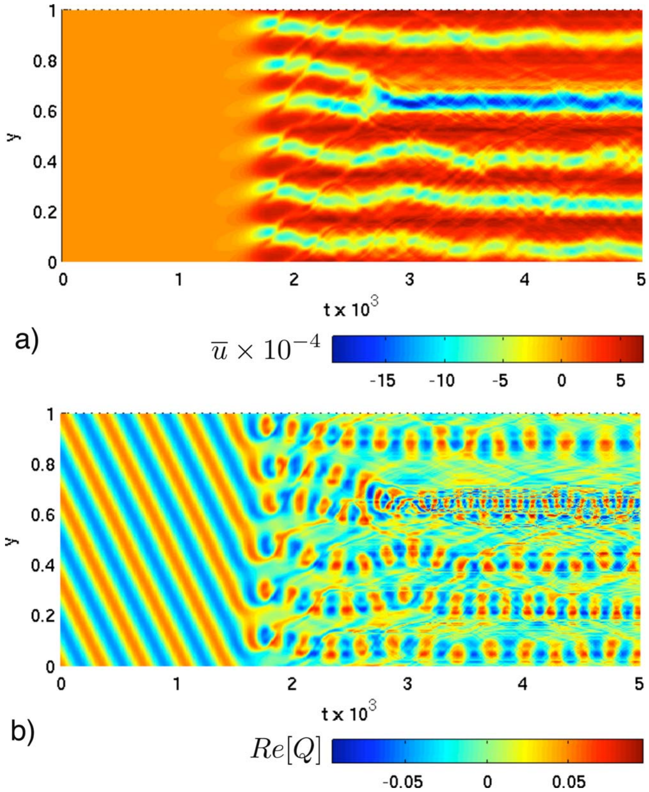


FIG. 10. (Color online) Space-time plot of (a) zonal velocity $\overline{u}$ and (b) disturbance vorticity component $\mathrm{Re}[Q]$ for a modulational instability simulation with $k_0=50$, $l_0=6\pi$, $\mathcal{N}_0=1.25\times 10^{-3}$, and $\beta=1$.

mode that is of *larger* wavenumber than that of the base planetary wave, $l_0$. Because of this, and the linearity assumption introduced after Eq. (32), it cannot be expected to remain valid after the initial growth phase. As an example, Fig. 10 shows a space-time plot of $\mathrm{Re}[Q]$ and $\overline{u}$ for a simulation that was allowed to continue for a long time after the onset of barotropic instability. As we are neglecting wave-wave interactions and restricting the wavefield to a single east-west wavenumber $k_0$, the results of this simulation cannot be assumed to be physically realistic. However, they were judged interesting enough to merit a brief discussion here.

The initial fastest growing zonal mode, which is clearly of different wavenumber from the base planetary wave, evolves rapidly after the barotropic instability criterion is broken (time $\approx 1750$). The expected east-west asymmetry quickly develops, and two of the growing jets can be seen to merge at time $\approx 2750$, with the resultant jet stronger than any of the others. The correlation between the zonal flow and the wavefield is extremely interesting; note that the jets appear to be trapping wavepackets, which propagate inside for the duration of the simulation in most cases. Calculation of the real-space wave action $n$ confirmed that the nonacceleration theorem was obeyed closely even to the end of the simulation.

Although idealized, this quasilinear study points the way toward more general investigations of jet formation via the modulational instability mechanism. In particular, it would be most interesting in future work to compare the predictions of Eq. (37) with (a) a wave-mean flow simulation that allows multiple east-west wavenumbers and (b) a fully nonlinear $\beta$-plane simulation.

## VI. DISCUSSION

We have studied the interaction between an arbitrary zonal flow and a broadband distribution of planetary waves. First, a new planetary wave Vlasov equation was derived that included all effects of the mean flow on the waves. A simple wave-mean flow numerical model was then used to investigate the interaction between planetary waves and zonal flow in a series of simple test cases. Jet formation and asymmetry were intuitively explained in terms of the motion of planetary wavepackets in phase space.

Next, the quasilinear instability of an initially monochromatic planetary wave was investigated. A generalization of the analysis of Manin and Nazarenko[10] was used to predict a finite fastest growing zonal wavenumber. This was then compared to the results of a number of numerical simulations for varying values of east-west wavenumber $k_0$. The prediction was found to give good agreement with numerical results for a wide range of parameter values. Jet asymmetry was again observed in the simulation (although in the opposite sense to that in the wavepacket example) and explained via a phase-space argument that made use of the results of Sec. IV.

The results presented here have demonstrated the effectiveness of the Wigner-based approach to wave-mean flow analysis. While previous studies have noted the possibility of $\beta$-plane modulational instability and estimated a time scale for the growth rate when it occurs, this appears to be the first work in which a fastest growing zonal mode for an arbitrary planetary wave is predicted and the results tested against a more general numerical simulation.

It is quite possible that planetary wave modulational instability is an important mechanism for multiple jet formation in real planetary atmospheres and oceans. However, many of the assumptions used in this paper do not apply in more realistic scenarios. To investigate the importance of the mechanism further, therefore, it would be interesting to generalize the analysis presented here in several ways.

One of the main assumptions made in the Vlasov equation derivations is that scale separation exists between the mean flow and waves. Some progress has been made in generalizing beyond this assumption. For example, in Ref. 25, the scattering of waves off random topography in the absence of a mean flow was studied using an expansion of a Wigner transport equation to first order. They successfully used their method to derive transport equations for planetary waves propagating in a two-layer model with random topography included. Unfortunately, the presence of a finite-amplitude zonal flow in the system appears to make progress in this direction more difficult.

Given the correspondence between the scale-separated predictions and more general numerical simulation in this paper, however, this generalization may not be of primary importance. Perhaps more limiting is the restriction to wave-mean flow interactions only, which was used throughout the analysis. Wave-wave and turbulent interactions can play a very important role in the overall development of fluid flows on the $\beta$-plane, and any eventual general theory should aim to take them into account.

This generalization may not be easy either, as standard techniques for the derivation of wave-kinetic equations appear inapplicable in situations where the zonal flow is of finite amplitude.[10] It is possible that an extension of the operator-based derivation of Sec. III could be used to tackle this problem. As a first step, however, it would be interesting and relatively simple to compare the theoretical and numerical results presented here with a fully nonlinear numerical simulation.

## ACKNOWLEDGMENTS

The author would like to thank his supervisor, Professor P. L. Read, and also Professor D. G. Andrews, for helpful suggestions and advice on a draft version of this paper. The Wigner distribution plots were created using a modified version of a MATLAB script, the original of which is freely available online at http://page.mi.fu-berlin.de/burkhard/WavePacket/. This work was funded by a Natural Environments Research Council studentship.

[1] N. A. Maximenko, B. Bang, and H. Sasaki, "Observational evidence of alternating zonal jets in the world ocean," Geophys. Res. Lett. **32**, L12607, DOI:10.1029/2005GL022728 (2005).
[2] P. H. Diamond, S.-I. Itoh, K. Itoh, and T. S. Hahm, "Zonal flows in plasma: A review," Plasma Phys. Controlled Fusion **47**, R35 (2005).
[3] P. B. Rhines, "Waves and turbulence on a beta-plane," J. Fluid Mech. **69**, 417 (1975).
[4] K. Stewartson, "The evolution of the critical layer of a Rossby wave," Geophys. Astrophys. Fluid Dyn. **9**, 185 (1977).
[5] T. Warn and H. Warn, "The evolution of a nonlinear critical level," Stud. Appl. Math. **59**, 37 (1978).
[6] P. D. Killworth and M. E. McIntyre, "Do Rossby-wave critical layers absorb, reflect, or over-reflect?" J. Fluid Mech. **161**, 449 (1985).
[7] J. G. Charney and P. G. Drazin, "Propagation of planetary-scale disturbances from the lower into the upper atmosphere," J. Geophys. Res. **66**, 83, DOI:10.1029/JZ066i001p00083 (1961).
[8] D. G. Andrews and M. E. McIntyre, "Planetary waves in horizontal and vertical shear: The generalised Eliassen–Palm relation and the mean zonal acceleration," J. Atmos. Sci. **33**, 2031 (1976).
[9] A. I. Dyachenko, S. V. Nazarenko, and V. E. Zakharov, "Wave-vortex dynamics in drift and $\beta$-plane turbulence," Phys. Lett. A **165**, 330 (1992).
[10] D. Y. Manin and S. Y. Nazarenko, "Nonlinear interaction of small-scale Rossby waves with an intense large-scale zonal flow," Phys. Fluids **6**, 1158 (1994).
[11] J.-P. Laval, B. Dubrulle, and S. Nazarenko, "Dynamical modeling of subgrid scales in 2D turbulence," Physica D **142**, 231 (2000).
[12] R. Salmon, *Lectures on Geophysical Fluid Dynamics* (Oxford University Press, New York, 1998).
[13] D. G. Andrews, C. B. Leovy, and J. R. Holton, *Middle Atmosphere Dynamics* (Academic, New York, 1987).
[14] J. Pedlosky, *Geophysical Fluid Dynamics* (Springer, New York, 1987).
[15] A. Torre, *Linear Ray and Wave Optics in Phase Space* (Elsevier, New York, 2005).
[16] M. S. Longuet-Higgins and A. E. Gill, "Resonant interaction between planetary waves," Proc. R. Soc. London, Ser. A **299**, 120 (1967).
[17] P. H. Haynes, "On the instability of sheared disturbances," J. Fluid Mech. **175**, 463 (1987).
[18] A. Chekhlov, S. Orszag, S. Sukoriansky, B. Galperin, and I. Staroselsky, "The effect of small-scale forcing on large-scale structures in two-dimensional flows," Physica D **98**, 321 (1996).
[19] Y. Lee and L. M. Smith, "On the formation of geophysical and planetary zonal flows by near-resonant wave interactions," J. Fluid Mech. **576**, 405 (2007).
[20] A. C. Newell, "Rossby wave packet interactions," J. Fluid Mech. **35**, 255 (1969).
[21] A. E. Gill, "The stability of planetary waves on an infinite beta-plane," Geophys. Astrophys. Fluid Dyn. **6**, 29 (1974).
[22] J. G. Esler, "Benjamin–Feir instability of Rossby waves on a jet," Q. J. R. Meteorol. Soc. **130**, 1611 (2004).
[23] A. J. Manfroi and W. R. Young, "Slow evolution of zonal jets on the beta plane," J. Atmos. Sci. **56**, 784 (1999).
[24] G. I. Sivashinsky, "Weak turbulence in periodic flows," Physica D **17**, 243 (1985).
[25] J. M. Powell and J. Vanneste, "Transport equations for randomly perturbed Hamiltonian systems, with application to Rossby waves," Wave Motion **42**, 289 (2005).